Fabrication and characterization of aluminum oxide/chromium oxide superlattice for attenuated phase-shifting mask working at 193 nm wavelength

F.D. Lai*, L.A. Wang

Department of Electrical Engineering and Institute of Electro-Optical Engineering, National Taiwan University, Taipei, Taiwan, ROC

Abstract

Al_2O_3/Cr_2O_3 superlattices with dense structures are successfully deposited on UV grade fused silica substrates and Si wafers by r.f. reactive unbalanced magnetron sputtering in a mixture of argon and oxygen gases at 150 °C. The dependence of the optical constant, plasma induced spectral intensity and deposition rate on the deposition parameters such as oxygen flow rate and r.f. sputtering power are examined. It was found that when O_2 gas flow rate increases, the deposition rate and absorption of Al_2O_3 and Cr_2O_3 thin films decrease. The O/Cr ratio of the CrO_x thin films identified by X-ray photoelectron spectroscopy (XPS) ranges from 1.5 to 3.0 when the sputtering power of the Cr target is increased from 20 to 80 W. The optical constants of Al_2O_3/Cr_2O_3 superlattices and Al_2O_3 and Cr_2O_3 thin films are determined from the measured transmittance and reflectance by employing the reflection–transmittance (R–T) method. As for an attenuated phase-shifting mask (APSM) blank, it is found that when the thickness percentages of Al_2O_3 in Al_2O_3/Cr_2O_3 superlattices are set between 60% and 70% the optical constants of superlattices can be tuned within the required R–T domain. Chemical and adhesion requirements of Al_2O_3/Cr_2O_3 superlattices for APSM applications are also met. © 2002 Elsevier Science B.V. All rights reserved.

Keywords: Optical properties; Aluminium oxide; Chromium oxide; Physical vapor deposition

1. Introduction

ArF based photolithography employing advanced resolution enhancement technologies such as phase-shifting mask [1], off-axis illumination [2] and optical proximity correction [3] can achieve patterns with dimension of less than 100 nm. Owing to destructive optical interference of light at the edges of circuit features, a phase-shifting mask improves depth of focus and resolution [4]. Since an attenuated phase-shifting mask (APSM) can overcome phase conflict problems for arbitrary mask patterns [5] and can be more easily fabricated than the other types of PSMs, it has attracted much attention in industry. Generally, the key requirements for an APSM blank are: (1) 180° phase shift; (2) transmittance in the range of 4–15%; (3) reflectance less than 15%; (4)

surface roughness less than 3 nm after the chemical durability test; and (5) good adhesion [6].

A multi-layer film having the property of very thin layers with a periodicity of less than 10% of a working wavelength is called a superlattice, and shall satisfy the effective medium theory [7]. Optical properties of such a superlattice are less sensitive to the details of layer interfaces [8]. As for materials, aluminum oxide [9] and chromium oxide [10] thin films exhibit very good properties such as chemical inertness, mechanical strength, hardness and optical characteristics; therefore, they have been widely used in many applications such as corrosion protection, wear resistance, electronics, and optics. However, they have not been reported for being used as APSM layers in the ArF lithography. In this work, we demonstrate that a new Al_2O_3/Cr_2O_3 superlattice whose dielectric constants are tunable can be used as an APSM blank layer for working at 193 nm wavelength.

*Corresponding author. Tel.: +886-2-2363-5251; fax: +886-2-2593-6897.

E-mail address: fdlai@ttu.edu.tw (F.D. Lai).

During the deposition process the plasma-induced emission spectra were monitored in situ in order to study the effect of each deposition parameter which might determine the final optical property and deposition rate of the aluminum oxide and chromium oxide thin films. As such, the Al_2O_3/Cr_2O_3 superlattice prepared at the optimal deposition parameters are aimed to meet the optical, chemical and adhesion requirements of an APSM.

We report four main aspects in this paper:

1. the dependences of optical constant, plasma-induced spectral intensity and deposition rate on the deposition parameters such as oxygen flow rate and r.f. sputtering power of Al_2O_3 and Cr_2O_3 thin films are studied;
2. the refractive index n and the extinction coefficient k of Al_2O_3/Cr_2O_3 superlattice deposited at the optimal conditions for Al_2O_3 and Cr_2O_3 thin films are characterized;
3. the thickness percentage ranges of Al_2O_3 layer in Al_2O_3/Cr_2O_3 superlattices that meet the optical requirements of APSM are experimentally obtained; and
4. the compositions of Al_2O_3/Cr_2O_3 superlattices are characterized by the utilizing X-ray photoelectron spectroscopy (XPS). We also use atomic force microscopy (AFM) to study the surface roughness before and after chemical treatments and use Scotch tape to test adhesion.

2. Experiment

Al_2O_3, Cr_2O_3 and Al_2O_3/Cr_2O_3 superlattice thin films are deposited on UV grade fused silica substrates and also on polished Si wafers by using dual-gun r.f. reactive unbalanced magnetron sputtering in a mixture of argon and oxygen gases. Since a higher ion density can be obtained for an unbalanced magnetron sputtering system than a balanced one [11], a more dense thin film can be obtained. The substrates are rotated during the deposition process to obtain uniform thin films. The substrates are cleaned in an ultrasonic bath by a series of processes: in trichlorethane for 5 min, distilled ion (DI) water for 10 min, acetone for 5 min, DI water for 10 min, ethanol for 5 min and DI water for 10 min. Target materials are chromium (99.99% purity) and aluminum (99.999% purity). A deposition chamber surrounded by the heating girdles is evacuated to a base pressure of less than 1×10^{-6} torr using a cool trap and a diffusion pump. Prior to deposition the target is pre-sputtered for 20 min at 10 mtorr Ar pressure to remove AlO_x or CrO_x contaminants from the target erosion track, and for 1 h in the deposition parameters of the film deposited to poison the target surface and to fix the deposition rate and the property of the film. The substrate temper-
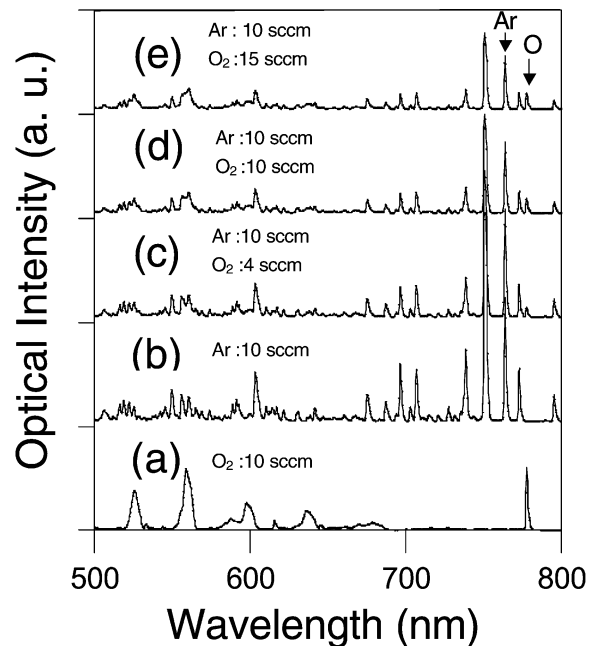

Fig. 1. Plasma induced emission spectra of excited argon and oxygen atoms at the gas flow rates of: (a) O_2 10 sccm only, (b) Ar 10 sccm only, (c) Ar 10 sccm and O_2 4 sccm, (d) Ar 10 sccm and O_2 10 sccm, and (e) Ar 10 sccm and O_2 15 sccm.

ature is controlled at 150 ± 1 °C. The gas flow rate measured with the accuracy better than 0.1 sccm is controlled by the mass flow meter. The Ar flow rate is kept constant at 10 sccm in all deposition processes while the O_2 flow rate is kept between 0 and 20 sccm. The O_2 gas inlet rings with 0.5 mm holes per cm is placed around the Al and Cr targets and the O_2 flow rate ratio for Al and Cr targets is set at $\sim 1:4$. The deposition parameters of the thin films are controlled by the gas pressure, gas flow rate and r.f. sputtering power. The plasma-induced emission of excited argon and oxygen atoms are characterized in situ by using a spectrometer, and the spectra are shown in Fig. 1. The significantly isolated wavelength peaks at 763.4 and 777.2 nm are from excited argon and oxygen atoms [12], respectively. The refractive index n, extinction coefficient k and deposition rates are analyzed and correlated with the two emission wavelengths. The film thickness is measured by using an AFM, and reflectance and transmittance are measured by an ex situ optical spectrometer (Hitachi, U3501), which has high photometric accuracy (better than 0.01%). The refractive index and extinction coefficient of each film at 193 nm wavelength is obtained by the reflection–transmittance (R–T) method in which the multiple reflection effect is taken into account [13]. Each Al_2O_3/Cr_2O_3 superlattice is composed of 10 Al_2O_3/Cr_2O_3 film stacks with ~ 9 nm, i.e. less than $\lambda/10$ thickness, in each stack. Each

layer's thickness in the stack is controlled by deposition rate and time; therefore, the chemical compositions of Al_2O_3/Cr_2O_3 superlattices can be determined. The chemical compositions of Al_2O_3 and Cr_2O_3 thin films are identified by utilizing XPS. An AFM is also used for the characterization of surface roughness before and after chemical durability measurement. The chemical durability of an Al_2O_3/Cr_2O_3 superlattice is measured in the 90 °C solution (90% 10M H_2SO_4 + 10% H_2O_2) for 1 h and then in another 50 °C solution (1 M KOH) for 30 s. The adhesion between the Al_2O_3/Cr_2O_3 superlattice and the UV grade fused silica is analyzed by using Scotch tape.

3. Experiment results

The experiment errors of deposition rate, refractive index and extinction coefficient are less than 5%. However, the experiment errors of optical intensity are less than 10%.

3.1. Deposition and optical property of Al_2O_3 and Cr_2O_3 thin films

To understand the influence of plasma process on deposition rate and optical property of Al_2O_3 and Cr_2O_3 thin films, the plasma-induced emission spectra of excited argon and oxygen atoms are monitored during the deposition as mentioned previously.

3.1.1. Effects of O_2 flow rate on Al_2O_3 thin films

The total chamber pressure and the Ar gas flow rate are, respectively, set at 8 mtorr and 10 sccm and the O_2 gas flow rate varies from 0 to 20 sccm. Fig. 1 shows that as O_2 flow rate increases the plasma-induced emission intensity of excited Ar atoms becomes markedly lower and that of excited O atoms becomes higher. Fig. 2a shows that the deposition rate of Al_2O_3 film depends on the plasma-induced emission intensity of excited Ar atoms, but not on the intensity of excited O atoms because the sputtering rate of the Ar plasma is higher than that of the O one. When the O_2 flow rate increases, the partial pressure of Ar decreases and the oxide layer on the target surface is thicker. Therefore, it is seen that as the O_2 flow rate increases, the Ar plasma intensity and the deposition rate become decreased. Since the probability of Al and O ions combination and the poison effect of O atoms on the Al target surface are higher at larger O_2 partial pressure, the extinction coefficient becomes lower and the refractive index higher as shown in Fig. 2b. The variations of the extinction coefficients and the refractive indices are small as the O_2 flow rate exceeds 10 sccm since Al is completely oxidized.
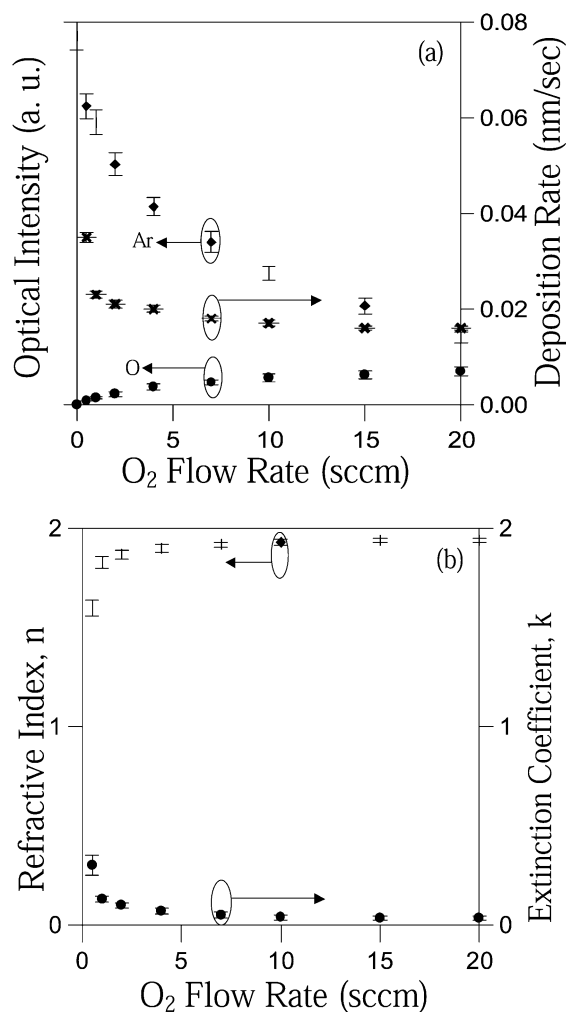

Fig. 2. (a) Variations of plasma induced emission intensities of excited Ar and O atoms and deposition rate of Al_2O_3 films with O_2 flow rates. (b) Optical constants variation of Al_2O_3 films with O_2 flow rates.

3.1.2. Effects of sputtering power on Al_2O_3 thin films

Fig. 3a depicts that plasma-induced emission intensities of excited Ar and O atoms and the deposition rates of the films increase with sputtering power. The amounts of excited Ar and O atoms that bombard the Al target are increased significantly at high sputtering power; the deposition rate is therefore increased.

It is well known that the deposition of films depends on the diffusion rate when constituent particles strike a substrate [14]. When the diffusion rate is not high enough, voids are generated in the films. The diffusion rate of the particles is related to the sputtering power and the deposition pressure. Due to the diffusion rate being not high enough, the refractive index and extinction coefficient of Al_2O_3 films are lower at 50 W sputtering power than those at 85 W as shown in Fig. 3b. The structure of Al_2O_3 film at 50 W is therefore not
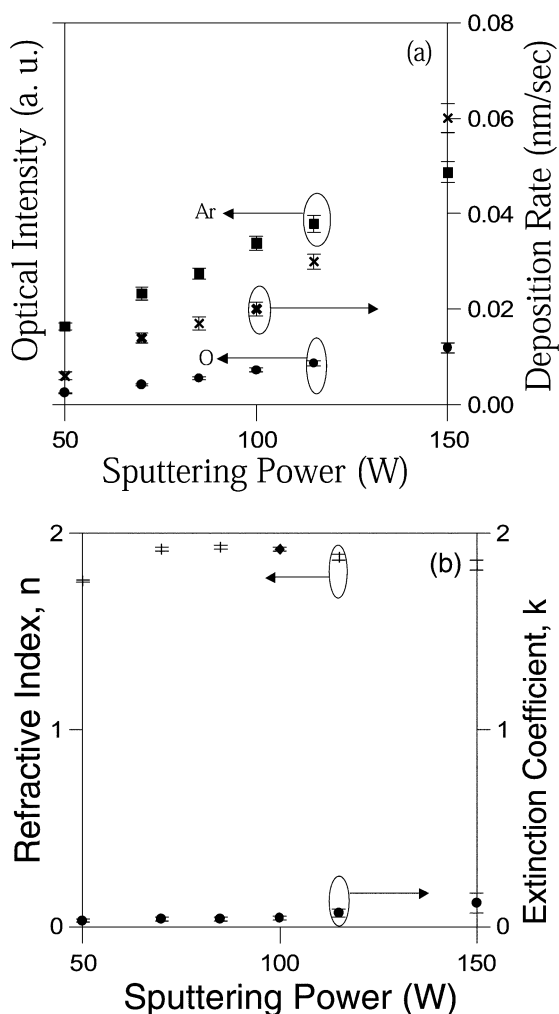
deposition pressure and the extinction coefficient has a minimum at ~8 mtorr.

3.1.4. Plasma-induced emission intensity, deposition rate, and dielectric constant of Cr_2O_3 thin films

The characteristics of plasma induced emission intensities of excited Ar and O atoms, deposition rate, optical constants of a Cr_2O_3 thin film are similar to those of an Al_2O_3 thin film as mentioned previously except for the sputtering power. Fig. 5 depicts that the extinction coefficient at 193 nm wavelength at 20 W sputtering power is lower than at higher sputtering power.

3.2. Chemical composition analysis of Al_2O_3 and Cr_2O_3 thin films by XPS

The ratio of O/Al in the Al_2O_3 thin film identified by XPS is 1.5 in the following deposition parameters: 8 mtorr pressure, 85 W sputtering power, flow rates of 10
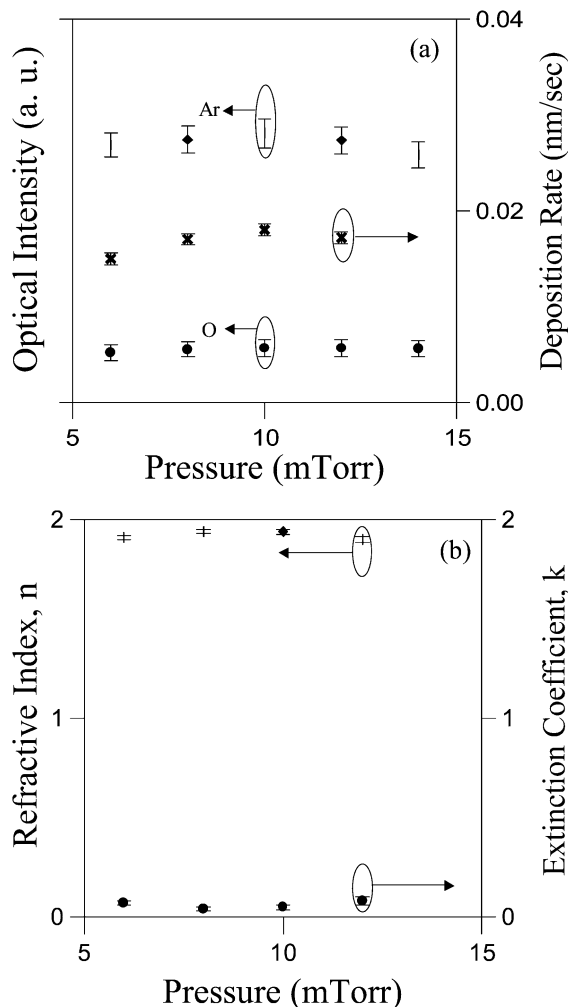

Fig. 3. (a) Variations of plasma induced emission intensities of excited Ar and O atoms and deposition rate of Al_2O_3 films with r.f. sputtering power. (b) Optical constant variation of Al_2O_3 films with r.f. sputtering power.

Fig. 4. (a) Variations of plasma induced emission intensities of excited Ar and O atoms and deposition rate of Al_2O_3 films with total gas pressure. (b) Optical constant variation of Al_2O_3 films with total process pressure.

dense. However, the high deposition rate at high sputtering power causes impurities and loose structures in the films [15]. As shown in Fig. 3b, the extinction coefficient of Al_2O_3 film is higher at 150 W sputtering power than that at 85 W due to some incompletely oxidized Al atoms left in the film.

3.1.3. Effects of gas pressure on Al_2O_3 thin films

The gas flow rates for both Ar and O_2 are 10 sccm. When the gas pressure increases, the atom's densities in the deposition chamber increase; therefore, the excited Ar and O atoms bombarding the target increase and their mean free paths decrease. Accordingly, plasma-induced emission intensities of excited Ar and O atoms and the deposition rate first increase and then decreases as shown in Fig. 4a. Fig. 4b depicts that the optical constants of Al_2O_3 films are dependent on the total
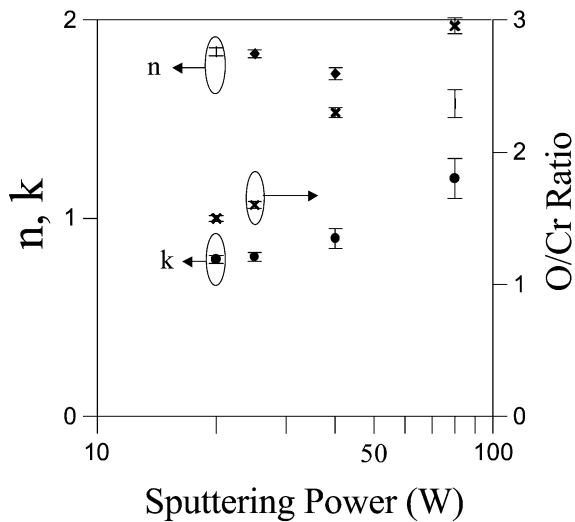
Fig. 5. Variations of optical constants and O/Cr ratios in CrO_x thin films with r.f. sputtering power.

sccm for Ar and 20 sccm for O_2. The rates of O/Al in the AlO_x thin film in other deposition parameters are slightly less than 1.5. At the same deposition parameters, the ratio of O/Cr in the CrO_x thin film identified by XPS ranges from 1.5 to 3.0 when the sputtering power in the Cr target is increased from 20 to 80 W as shown in Fig. 5. The chemical composition of CrO_3 at higher sputtering power forms easier than at lower sputtering power. The CrO_3 thin film deposited at 80 W sputtering power is unstable.

3.3. Optical property of Al_2O_3/Cr_2O_3 superlattices

Superlattices are deposited at the same deposition parameters except that 85 W sputtering power is used for the Al target and 20 W for the Cr target.

The superlattice optical constants are calculated by modeling the multi-layer with a single homogeneous thin film. Fig. 6a depicts that the optical constants of Al_2O_3/Cr_2O_3 superlattices are within the desired domain, i.e. transmittance between 4 and 15% and reflectance less than 15%, when the thickness percentage of Al_2O_3, which is defined as the ratio of Al_2O_3 thickness in each stack thickness [16], is set between 60 and 70%. Fig. 6b shows that the linear relationship of both real (n^2-k^2) and imaginary ($2nk$) parts of the dielectric constant with the thickness percentage of Al_2O_3 is verified and thus the dielectric constants of Al_2O_3/Cr_2O_3 superlattices satisfy the effective medium theory. Al_2O_3/Cr_2O_3 superlattices with tunable dielectric constants can then be easily used to design a desirable APSM blank. It has been reported that APSMs with 8–10% high transmittance would minimize the side-lobe effect [17]. When the Al_2O_3/Cr_2O_3 superlattice used as the APSM of 10% high transmittance and π-phase shift,

the calculated optimal thickness percentage of Al_2O_3, reflectance and total thickness of the superlattices are 64.5%, 10.2% and 111.5 nm, respectively.

3.4. Surface roughness and transmittance variation of Al_2O_3/Cr_2O_3 superlattices before and after chemical durability test

3.4.1. Surface roughness

The surface roughness of the films before and after chemical durability test are measured by using an AFM. Fig. 7a shows the results for a surface within a 1×1 μm^2 area before the chemical durability test, and Fig. 7b shows after. The root mean square value of the
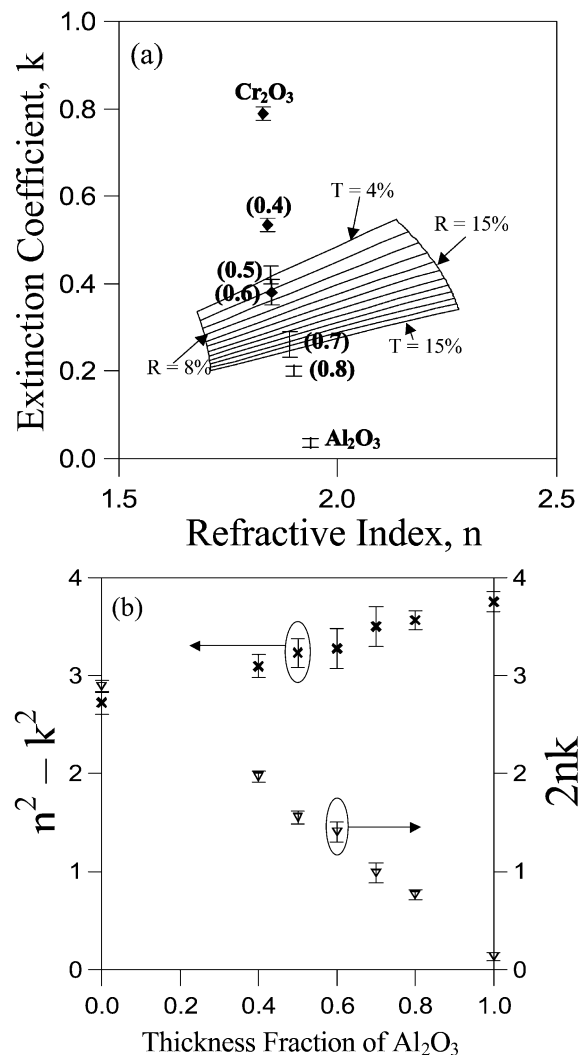

Fig. 6. (a) Calculated domain of desired optical constants and measured ones with various thickness percentage of Al_2O_3 in the Al_2O_3/Cr_2O_3 superlattice stacks. Indicated in parentheses are the thickness percentages of Al_2O_3 in the Al_2O_3/Cr_2O_3 superlattice stacks. (b) Variations of real (n^2-k^2) and imaginary ($2nk$) parts of dielectric constants of Al_2O_3/Cr_2O_3 superlattices with thickness percentage of Al_2O_3.

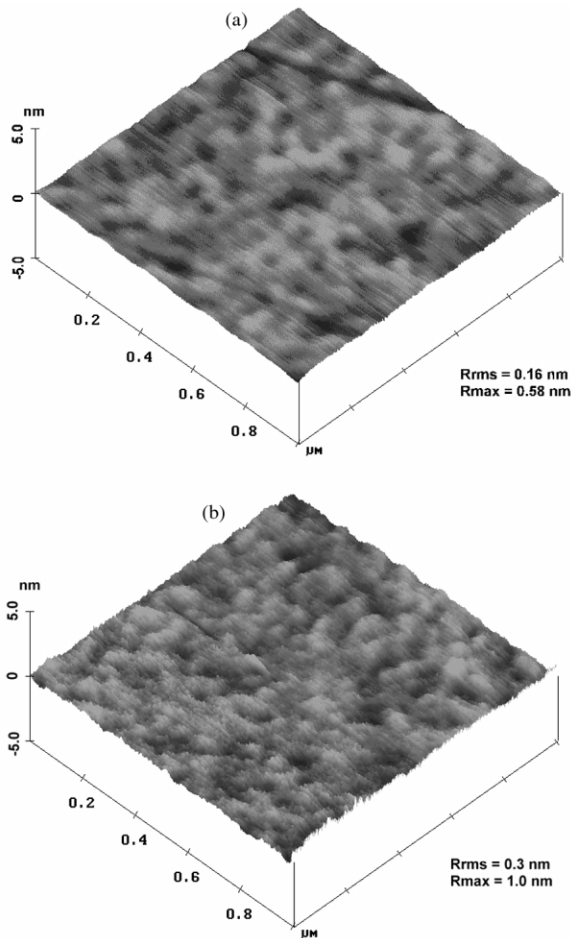Fig. 7. Surface roughness of Al_2O_3/Cr_2O_3 superlattice (a) before and (b) after the chemical durability test.

surface roughness before the test is less than 0.5 nm and the maximum peak to peak magnitude is less than 1 nm. After the test, the mean value is less than 1 nm and the maximum less than 2 nm. Accordingly, the chemical corrosion rates of the Al_2O_3/Cr_2O_3 superlattices are small, and the calculated average phase shift decreases by less than $\sim 2°$, which is within the acceptable range for APSM applications [6]. This is because both Al_2O_3 and Cr_2O_3 thin films exhibit good chemical inertness.

3.4.2. Transmittance variation

After the chemical durability test, the transmittance of Al_2O_3/Cr_2O_3 superlattices increase less than 0.2%. This suggests that the film thickness decreases very little because Al_2O_3/Cr_2O_3 superlattices have high resistance to chemical corrosion, which is in consistency with the result described in Section 3.4.1.

3.5. Adhesion test of Al_2O_3/Cr_2O_3 superlattices by Scotch tape testing

The adhesions among the films and to the fused silica substrate are very important. An investigation using Scotch tape in the ASTM Crosshatch tape testing method [6] is carried out on the films deposited on fused silica substrates. All the films pass the adhesion test. The adhesion strengths of the films are so strong that the films still adhere well with the substrates even though they are scratched by the Scotch Brite scouring pad.

4. Conclusion

An Al_2O_3/Cr_2O_3 superlattice with tunable optical constants is a new material candidate for APSMs to be working at 193 nm wavelength. Al_2O_3 and Cr_2O_3 thin films and Al_2O_3/Cr_2O_3 superlattices with dense structures are successfully deposited on UV grade fused silica substrates and Si wafers by r.f. reactive unbalance magnetron sputtering. It is found that deposition rates of the films are linearly proportional to the plasma-induced emission intensity of excited Ar atoms. The higher the O_2 flow rates are, the lower the extinction coefficients, i.e. the oxidation of the films increases as evidenced by the plasma-induced emission intensity of excited O atoms. The ratios of O/Al in the AlO_x thin films identified by XPS are equal to or slightly less than 1.5 while the ratios of O/Cr in the CrO_x thin films ranges from 1.5 to 3.0 when the sputtering power is increased from 20 to 80 W. The extinction coefficient of thin film at 193 nm wavelength at 20 W sputtering power is lower than at higher sputtering power. Al_2O_3 and Cr_2O_3 thin films deposited by employing the optimal deposition parameters are stoichiometric. Optical properties of Al_2O_3/Cr_2O_3 superlattices can be tuned by controlling the thickness percentage of Al_2O_3 in Al_2O_3/Cr_2O_3 stacks. The optical constants are shown to be within the desired reflectance–transmittance domain when the thickness percentage of Al_2O_3 in Al_2O_3/Cr_2O_3 superlattices is set between 60% and 70%. Al_2O_3/Cr_2O_3 superlattices with tunable optical constant can be easily used as a desirable material blank for APSM. The dielectric constants of Al_2O_3/Cr_2O_3 superlattices are shown to fit the effective medium theory. And the calculated optimal thickness percentage of Al_2O_3 in the Al_2O_3/Cr_2O_3 superlattice used as APSM of 10% transmittance, with minimum side-lobe effect, and π-phase shift is 64.5%. Before and after the chemical durability test, the calculated average phase shift of the superlattices decreases by less than $\sim 2°$, which is within the acceptable range for APSM applications. Strong adhesion strengths among Al_2O_3/Cr_2O_3 superlattice layers and to the UV grade fused silica substrates are obtained.

References

[1] M.D. Levenson, R.A. Simpson, IEEE Trans. Electron Devices 29 (1982) 1828.

[2] M. Noguchi, M. Muraki, Y. Iwasaki, A. Suzuki, SPIE 1674 (1992) 741.

[3] A. Starikov, SPIE 1088 (1989) 34.

[4] H. Watanabe, E. Sugiura, Y. Todokoro, M. Inoue, Jpn. J. Appl. Phys. 30 (1991) 3004.

[5] T. Terasawa, N. Hasegawa, H. Fukuda, S. Katagiri, Jpn. J. Appl. Phys. 30 (1991) 2991.

[6] P.F. Carcia, R.H. French, K. Sharp, J.S. Meth, B.W. Smith, SPIE 2884 (1996) 255.

[7] O. Hunderi, Physica A 157 (1989) 309.

[8] O. Hunderi, J. Wave-Mater. Interact. 2 (1987) 29.

[9] E. Dörre, H. Hubner (Eds.), Alumina: Processing Properties and Applications, Springer, Berlin, 1984.

[10] P. Hones, M. Diserens, F. Lèvy, Surf. Coat. Technol. 120–121 (1999) 277.

[11] W.D. Sproul, Surf. Coat. Technol. 49 (1991) 284.

[12] R. Payling, D.G. Jones, A. Bengtson, Glow Discharge Optical Emission Spectrometry, 1997.

[13] T.C. Paulick, Applied Optics 25 (4) (1986) 562.

[14] J.A. Thornton, J. Vac. Sci. Technol. A. 4 (6) (1986) 3059.

[15] J.P. Bucher, K.P. Ackermann, F.W. Buschor, Thin Solid Films 122 (1984) 63.

[16] P.F. Carcia, R.H. French, M.H. Reilly, M.F. Lemon, D.J. Jones, Appl. Phys. Lett. 70 (1997) 2371.

[17] Z. Cui, P.D. Prewett, S. Johnson, Microelectron. Eng. 27 (1995) 259.